Rapid Reports

Trapping the $P^+B_L^-$ Initial Intermediate State of Charge Separation in Photosynthetic Reaction Centers from *Rhodobacter capsulatus*†

Brett Carter,‡ Steven G. Boxer,‡ Dewey Holten,§ and Christine Kirmaier*,§

Department of Chemistry, Stanford University, Stanford, California 94305-5080, and Department of Chemistry, Washington University, St. Louis, Missouri 63130-4899

Received February 18, 2009

ABSTRACT: The short-lived (<1 ps) initial intermediate state $P^+B_L^-$ in the photoinduced charge separation process of the bacterial photosynthetic reaction center has been trapped in two D_{LL}-based *Rhodobacter capsulatus* mutants that have Tyr at position M208 and lack the bacteriopheophytin electron acceptor H_L. Transient state $P^+B_L^-$ is characterized by a 1017 nm bacteriochlorophyll anion absorption band and decays by charge recombination with a lifetime of several hundred picoseconds at 295 K. $P^+B_L^-$ is not observed in an otherwise identical mutant that has Phe at M208, which appears to make the state thermodynamically inaccessible from the excited primary electron donor P*.

The bacterial photosynthetic reaction center (RC)[1] converts light energy into chemical potential energy via rapid, multistep, membrane-spanning charge separation. This process is initiated by excitation of a bacteriochlorophyll dimer (P) to its lowest singlet excited state (P*) and is mediated by a monomeric bacteriochlorophyll (B_L) and a bacteriopheophytin (H_L) via which an electron is delivered to a quinone (Q_A) on a subnanosecond time scale with essentially unity yield. B_L, H_L, and Q_A are primarily housed on the L subunit of the RC but also have interactions with the D helix of the M polypeptide (Figure 1); B_M, H_M, and Q_B are associated with the M subunit and the D helix of the L polypeptide in analogous positions related by a local C_2 axis of symmetry. Electron transfer (ET) does not occur from P* to the M side pigments in the native RC. The cofactor arrangement (*1*) is shown in Figure 1.

Figure 2A shows a working model for the energetics in wild-type (WT) RCs in which $P^+B_L^-$ is ~0.1 eV below P* and $P^+B_M^-$ is above P* in free energy (*2*−*11*). Two residues that are particularly important in this energy ordering are symmetry-related Phe L181 and Tyr M208 that flank P and are near B_M and B_L, respectively (Figure 1). Electrostatics calculations have suggested that there are two dominant orientations of the hydroxyl dipole of Tyr M208, one of which stabilizes B_L^-, and that B_M^- is not similarly stabilized by the adjacent Phe at L181 (*2, 5*). If $P^+B_M^-$ is poised more than ~25 meV above P*, ET to the M branch to produce $P^+H_M^-$ can occur only via a superexchange mechanism in which $P^+B_M^-$ is a virtual intermediate. This process cannot compete effectively with a faster P* → $P^+B_L^-$ → $P^+H_L^-$ two-step process on the L branch (*11*) in which formation of $P^+B_L^-$ as a chemical intermediate is thermodynamically possible.

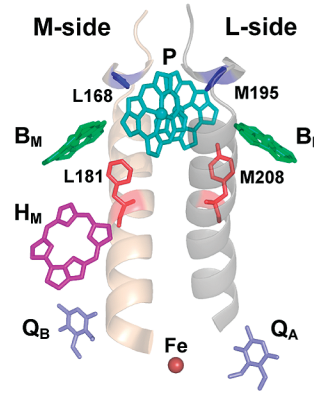

RC	L168	L181	M195	M208
WT	H	F	F	Y
D_{LL}	H	F	H	F
D_{LL}-1	F	Y	F	F
D_{LL}-2	F	F	F	Y
D_{LL}-3	F	Y	F	Y
D_{LL}-4	F	F	F	F

FIGURE 1: RC cofactors, D helices of the L and M polypeptides, and key amino acid residues whose substitutions in the D_{LL} mutant background are summarized in the chart on the right. H_L at the position related to H_M by the local C_2 axis of symmetry is absent in the mutants that are the focus of this study.

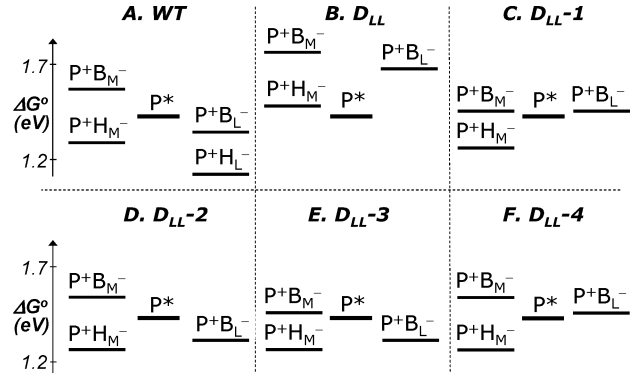

FIGURE 2: Models for the free energies of the charge-separated states in the RCs indicated. States $P^+Q_A^-$ and $P^+Q_B^-$ (not shown) are at ~0.6 eV relative to the ground state.

† This work was supported by the National Science Foundation (Grant MCB-0416623 to S.G.B. and Grant MCB-0614529 to D.H. and C.K.).

* To whom correspondence should be addressed. E-mail: kirmaier@wustl.edu. Phone: (314) 935-6480. Fax: (314) 935-4481.

‡ Stanford University.

§ Washington University.

[1] Abbreviations: RC, reaction center; ET, electron transfer; WT, wild type; BChl, bacteriochlorophyll; B_L and B_M, monomeric BChls on the L and M branches, respectively; H_L and H_M, monomeric bacteriopheophytins on the L and M branches, respectively; Deriphat-Tris buffer, 0.05% Deriphat 160-C/10 mM Tris, pH 8.0/300 mM NaCl.

10.1021/bi900282p CCC: $40.75
Published on Web 02/26/2009

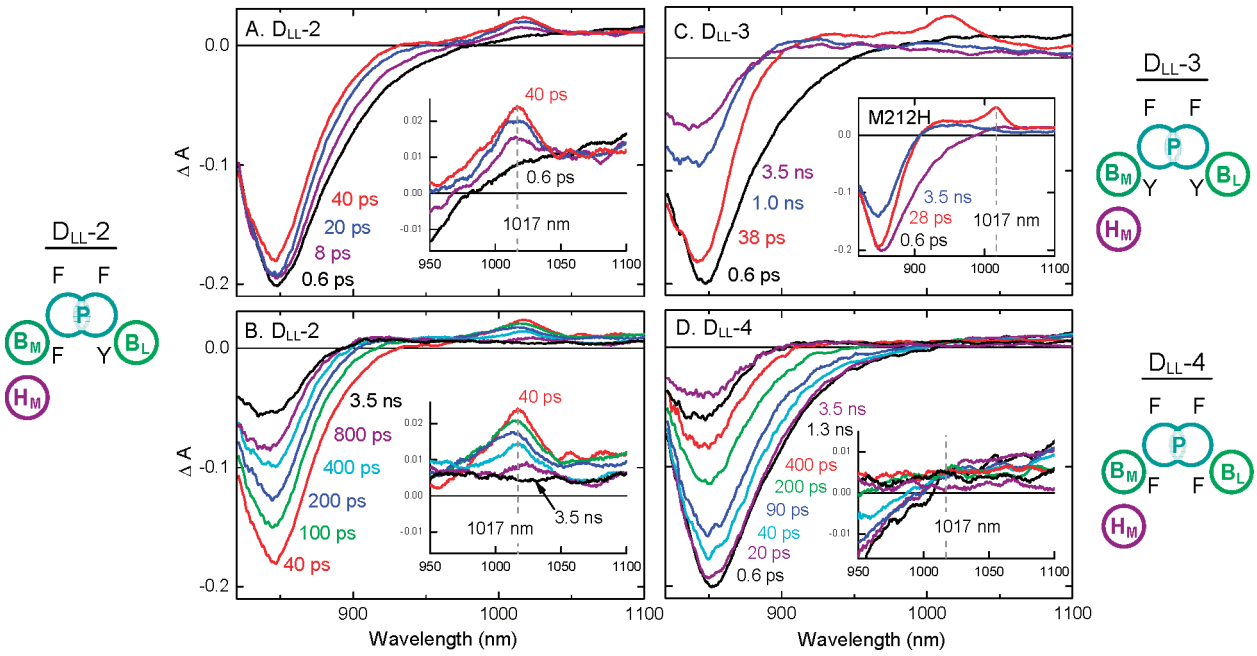

FIGURE 3: Transient absorption spectra of RCs in Deriphat-Tris buffer[1] at 295 K acquired after a 130 fs excitation flash at 600 nm using methods described in refs *9* and *15*. The insets in panels A, B, and D expand the views of the 950−1100 nm region of the spectra in the main panels. The inset in panel C shows data for the M212H mutant used for comparison. The black letters in the cartoons denote the amino acids at (clockwise from top left) L168, M195, M208, and L181 as per Figure 1.

In WT RCs, P* has a lifetime of 3−4 ps and $P^+B_L^-$ has a lifetime of ~0.7 ps. Thus, the transient population of $P^+B_L^-$ in the two-step sequence is at most only 10−20% of the initial P* concentration (*11*). Trapping $P^+B_L^-$ and probing its inherent dynamics would be of considerable interest because of its key role in the mechanism and directionality of charge separation (*2*−*12*). This goal has been achieved herein using a strategy that involves (i) mutants based on the D_{LL} construct, which lacks the H_L cofactor, and (ii) modulating the energetics of initial ET by manipulation of the amino acids at L181 (near B_M) and M208 (near B_L).

In the D_{LL} mutant, M subunit D helix residues M192−M217 that contact P, B_L, and H_L are replaced with L subunit D helix residues L165−L190, resulting in 12 amino acid changes from WT (*13, 14*). Detergent-isolated D_{LL} RCs (*15, 16*), like D_{LL} RCs in chromatophore membranes (*13*), are photochemically inactive: P* decays to the ground state in 100−200 ps with no evidence of the formation of any charge-separated state. This outcome is consistent with all of the charge-separated intermediates ($P^+B_L^-$, $P^+B_M^-$, and $P^+H_M^-$) being above P* in free energy (Figure 2B). This energy ordering arises because P in the D_{LL} mutant is at least 100 mV harder to oxidize than P in WT (*15*). The higher oxidation potential of P in D_{LL} derives in part from residues L168 and M195 both being His, whereas they are His and Phe, respectively, in WT. In an RC denoted D_{LL}-1 [D_{LL}-FY_LF_M in previous work (*15, 16*)], these two residues are both Phe and P is slightly easier to oxidize than in WT (P/P^+ midpoint potential of 475 mV vs 505 mV) (*15*). D_{LL}-1 has a Tyr at L181, which is believed to stabilize $P^+B_M^-$ (Figure 2). These three amino acid changes in D_{LL}-1 result in an RC that gives 70% charge separation to H_M from P* with the remaining 30% of P* deactivating to the ground state (*15*). The relatively slow, ~$(80\ ps)^{-1}$, rate of $P^+H_M^-$ formation in D_{LL}-1 at 295 K suggests that $P^+B_M^-$ remains above P* and facilitates ET via superexchange. Because there is no evidence that $P^+B_L^-$ forms in D_{LL}-1, it is presumed that this state remains above P* (Figure 2C). This hypothesis is consistent with residue M208 near B_L being Phe in the D_{LL} background and unable to afford the free energy stabilization of $P^+B_L^-$ that Tyr M208 provides in the WT RC.

D_{LL}-1 was designed from D_{LL} to facilitate ET to H_M. Here we follow a related logic with the goal of promoting L side ET to B_L with a Tyr at M208 and a Phe at L181 (D_{LL}-2). If $P^+B_L^-$ forms within a few picoseconds as in WT, then P* → $P^+B_L^-$ ET should completely dominate over M side ET. The same should also be true for D_{LL}-3, which has Tyr residues at both L181 and M208. Placement of Phe at both sites in D_{LL}-4 provides a control in which $P^+B_L^-$ formation should be inhibited, as it is in D_{LL}-1. Our initial results on these three new mutants definitively show that a P^+B^- state, assigned to $P^+B_L^-$ as described below, is trapped in D_{LL}-2 and D_{LL}-3, demonstrating the essential role of Tyr at M208. This state is not produced in D_{LL}-4 (compare panels D−F of Figure 2).

Panels A and B of Figure 3 show time-resolved absorption difference spectra of D_{LL}-2. The spectrum at 0.6 ps can be ascribed to P*, with characteristic bleaching of the near-infrared ground-state absorption band of P at ~850 nm and stimulated emission from P* on the long-wavelength side of the bleaching and extending to ~1000 nm. The P* stimulated emission decay displays fast (5−10 ps) and slow (~100 ps) components similar in amplitude. As the 5−10 ps component of the stimulated emission decays, a small but distinct absorption band at 1017 nm grows in, also with a time constant of 5−10 ps (Figure 3A and inset). The 1017 nm band decays with a time constant of 400−500 ps (Figure 3B and inset) and is accompanied by P bleaching decay at 850 nm. A similar time evolution of a 1017 nm band is observed for D_{LL}-3 (Figure 3C). We assign the absorption feature at 1017 nm to a bacteriochlorophyll (BChl) anion, and specifically to the B_L^- component of state $P^+B_L^-$. These assignments are described in the following.

An absorption feature in the 1010−1020 nm region has been attributed to B_L^- in WT and several mutants designed to affect

the rates of formation and/or decay of short-lived $P^+B_L^-$ (*3, 11*). Assignment of the clearly resolved 1017 nm band to a $BChl^-$ in D_{LL}-2 and D_{LL}-3 is further supported by formation of a very similar feature upon reduction of the BChl (denoted β) that replaces H_L in the M212H mutant (28 ps spectrum in the inset of Figure 3C) (*17*). Thus, $BChl^-$ in either the B_L or H_L binding site gives a distinct near-infrared absorption feature at 1017 nm. Similarly, the anion of BChl-*a* in vitro has a distinct absorption band at ~1000 nm (*18*).

In contrast to D_{LL}-2 and D_{LL}-3, a near-infrared $BChl^-$ band is not observed in the transient spectra of D_{LL}-4 (Figure 3D), and the P* stimulated emission decay kinetics do not have a 5−10 ps component. Instead, in D_{LL}-4, the P* stimulated emission kinetics are single exponential ($\tau \simeq 120$ ps). Similarly, a $BChl^-$ band is not observed for D_{LL}-1 (*15*). Both D_{LL}-1 and D_{LL}-4 have Phe near B_L at M208, whereas D_{LL}-2 and D_{LL}-3 have Tyr at this site. These collective findings readily lead to the assignment of the 1017 nm absorption band observed for D_{LL}-2 and D_{LL}-3 to the B_L^- constituent of $P^+B_L^-$. The formation of $P^+B_L^-$ in these two mutants implies that the Tyr at M208 sufficiently stabilizes $P^+B_L^-$ to make it thermodynamically accessible from P*. Apparently, the state lies above P* in D_{LL}-1 and D_{LL}-4, which instead have Phe at this site (Figure 2).

Because D_{LL}-2 and D_{LL}-3 lack H_L, $P^+B_L^-$ cannot decay by ET to give $P^+H_L^-$, but instead only by charge recombination, perhaps in part via thermal repopulation of P*. The $P^+B_L^-$ lifetime is several hundred picoseconds in both D_{LL}-2 and D_{LL}-3, which is much shorter than the lifetime of 10−20 ns of $P^+H_L^-$ in WT obtained when ET to Q_A is blocked (*19, 20*). This difference can be attributed in large measure to the shorter distance and thus stronger electronic coupling between P^+ and B_L^- than between P^+ and H_L^-. In a mutant where the His ligand of B_M is replaced with Glu, $P^+B_M^-$ is thought to form, lying below both P* and $P^+H_M^-$, and to have a charge recombination time constant of ~65 ps (*21*).

In D_{LL}-2, D_{LL}-3, and D_{LL}-4, P* also decays in part via M side ET to give $P^+H_M^-$, although in reduced yield compared to that of D_{LL}-1. Analysis of the complex, multiexponential, and probe wavelength-dependent kinetics found in these D_{LL}-based mutants (*16*) and comparisons of the rates and yields of formation of $P^+B_L^-$ and $P^+H_M^-$ will be reported in future work. A qualitative picture that emerges is that in both D_{LL}-2 and D_{LL}-3 there is a fast P* decay component (5−10 ps) associated with significant ET to B_L and a slower decay component (50−100 ps) associated with some ET to H_M and deactivation to the ground state. Obviously, the biexponential P*-stimulated emission decay and distinct time scales for formation of the different P* photoproducts in D_{LL}-2 and D_{LL}-3 cannot be explained by a simple competition between decay pathways from P*. Instead, there appear to be effectively different (nominally two) pigment−protein subpopulations that differ in activity and that do not interconvert on the time scale of the inherent (100−200 ps) P* lifetime. This has been described in detail previously for D_{LL}-1 at 77 K and other RCs containing a swap of Tyr M208 and Phe L181 (*16, 17, 22*). Such RC subpopulations may arise because the small free energy spacings among P*, $P^+B_L^-$, and $P^+B_M^-$ in WT are even smaller by design in these mutants (Figure 2). This makes the rates of ET to the L or M side, or the ability to perform ET at all, very sensitive to pigment−protein conformational effects. For example, the subpopulations may be distinguished by the specific orientation of the OH dipole of a Tyr at M208 (or L181) and thus the free energies of $P^+B_L^-$ (or $P^+B_M^-$).

In summary, we have provided compelling evidence of trapping of a state containing a reduced bacteriochlorophyll, proposed to be $P^+B_L^-$, in mutants D_{LL}-2 and D_{LL}-3 and its absence in D_{LL}-4. Rather than having the small (10−20%) transient population and ultrashort (<1 ps) lifetime exhibited in WT RCs, $P^+B_L^-$ in the new D_{LL}-based mutants has significant population, and its decay over several hundred picoseconds can be measured for the first time. The trapping of $P^+B_L^-$ in D_{LL}-2 and D_{LL}-3 but not in D_{LL}-4 or D_{LL}-1 was achieved by using Tyr and the associated hydroxyl dipole as an amino acid switch. $P^+B_L^-$ and its counterpart $P^+B_M^-$ are integral to the mechanisms and dynamics of charge separation on their respective electron transport chains and in determining the unidirectionality of charge separation via only the L branch in the WT RC. The results obtained herein open the door for detailed examination and manipulation of the properties of these two key charge-separated states and deeper scrutiny of how their roles in primary charge separation are controlled by protein environmental factors.

REFERENCES

1. Ermler, U., Fritsch, G., Buchanan, S. K., and Michel, H. (1994) *Structure 2*, 925–936.
2. Parson, W. W., Chu, Z. T., and Warshel, A. (1990) *Biochim. Biophys. Acta 1017*, 251–272.
3. Arlt, T., Schmide, S., Kaiser, W., Lauterwasser, C., Meyer, H., Scheer, H., and Zinth, W. (1993) *Proc. Natl. Acad. Sci. U.S.A. 90*, 11757–11761.
4. Bixon, M., Jortner, J., and Michel-Beyerle, M. E. (1995) *Chem. Phys. 197*, 389–404.
5. Alden, R. G., Parson, W. W., Chu, Z. T., and Warshel, A. (1996) *J. Phys. Chem. 100*, 16761–16770.
6. Gunner, M. R., Nicholls, A., and Honig, B. (1996) *J. Phys. Chem. 100*, 4277–4291.
7. Holzwarth, A. R., and Müller, M. G. (1996) *Biochemistry 35*, 11802–11831.
8. Shuvalov, V. A., and Yakovlev, A. G. (1998) *Biol. Membr. 15*, 455–460.
9. Kirmaier, C., He, C., and Holten, D. (2001) *Biochemistry 40*, 12132–12139.
10. Katilius, E., Babendure, J. L., Lin, S., and Woodbury, N. W. (2004) *Photosynth. Res. 81*, 165–180.
11. Zinth, W., and Wachtveitl, J. (2005) *ChemPhysChem 6*, 871–880.
12. Wakeham, M. C., and Jones, M. R. (2005) *Biochem. Soc. Trans. 133*, 851–857.
13. Breton, J., Martin, J. L., Lambry, J. C., Robles, S. J., and Youvan, D. C. (1990) in *Structure and Function of Bacterial Photosynthetic Reaction Centers* (Michel-Beyerle, M. E., Ed.) pp 293−302, Springer-Verlag, New York.
14. Robles, S. J., Breton, J., and Youvan, D. C. (1990) *Science 248*, 1402–1405.
15. Chuang, J. I., Boxer, S. G., Holten, D., and Kirmaier, C. (2006) *Biochemistry 45*, 3845–3851.
16. Chuang, J. I., Boxer, S. G., Holten, D., and Kirmaier, C. (2008) *J. Phys. Chem. B 112*, 5487–5499.
17. Kirmaier, C., and Holten, D. (2009) *J. Phys. Chem. B 113*, 1132–1142.
18. Fajer, J., Borg, D. C., Forman, A., Dolphin, D., and Felton, R. H. (1973) *J. Am. Chem. Soc. 95*, 2739–2741.
19. Ogrodnik, A., Keupp, W., Volk, M., Aumeier, G., and Michel-Beyerle, M. E. (1994) *J. Phys. Chem. 98*, 3432–3439.
20. Tang, C.-K., Williams, J. C., Taguchi, A. K. W., Allen, J. P., and Woodbury, N. W. (1999) *Biochemistry 38*, 8794–8799.
21. Katilius, E., Katiliene, Z., Lin, S., Taguchi, A. K. W., and Woodbury, N. W. (2002) *J. Phys. Chem. B 106*, 12344–12350.
22. Kirmaier, C., Laible, P. D., Hinden, E., Hanson, D. K., and Holten, D. (2003) *Chem. Phys. 294*, 305–318.

BI900282P